Adjustment of the position of the centre of rotation for the beams in the cryogenic suspension

Fabián Peña Arellano, et al.*

October 2023

1 Rigid body model calculation

This document reports the results of the adjustment of the centre of rotation of the suspension beams, when the centre of percussion is at the position of the upper flexure, more specifically, at its supporting face at its bottom.

The calculation relies on the rigid body model that has already been developed for an inverted pendulum, like the ones used in Virgo and KAGRA. In the current case, however, the centre of rotation has to coincide with the position of the lower mass, rather than with the position of the upper one. Fig. 1 shows on the left the diagram of an inverted pendulum. The description of the relevant symbols is give in Table 1.

Following Ref. [2, p. 49], the formulas determining the transfer function $H(s)$ from the displacement of the ground to the displacement of the upper body are:

$$H(s) = \frac{A - Bs^2}{A + Cs^2} \tag{1}$$

$$A = \frac{k_\theta}{L_1^2} - \frac{g}{L_1}\left(M + \frac{m_1}{2} - \frac{m_2 L_2}{2L_1} - \frac{M_3 L_2}{L_1}\right), \tag{2}$$

$$B = -\frac{I_1 + I_2}{L_1^2} + \frac{m_1}{4} - L_2 m_2\left(\frac{2L_1 + L_2}{4L_1^2}\right) - L_2 M_3\left(\frac{L_1 + L_2}{L_1^2}\right), \tag{3}$$

$$C = M + \frac{m_1}{4} + \frac{L_2^2 m_2}{4L_1^2} + \frac{L_2^2 M_3}{L_1^2} + \frac{I_1 + I_2}{L_1^2}, \tag{4}$$

where $s = i\omega$ is the Laplace variable and ω is the angular frequency. The resonant angular frequency and the saturation value of the attenuation are given respectively as

$$\omega_0 = \frac{A}{C}, \qquad \beta = \frac{B}{C}, \tag{5}$$

*We will add more names as the content becomes updated.

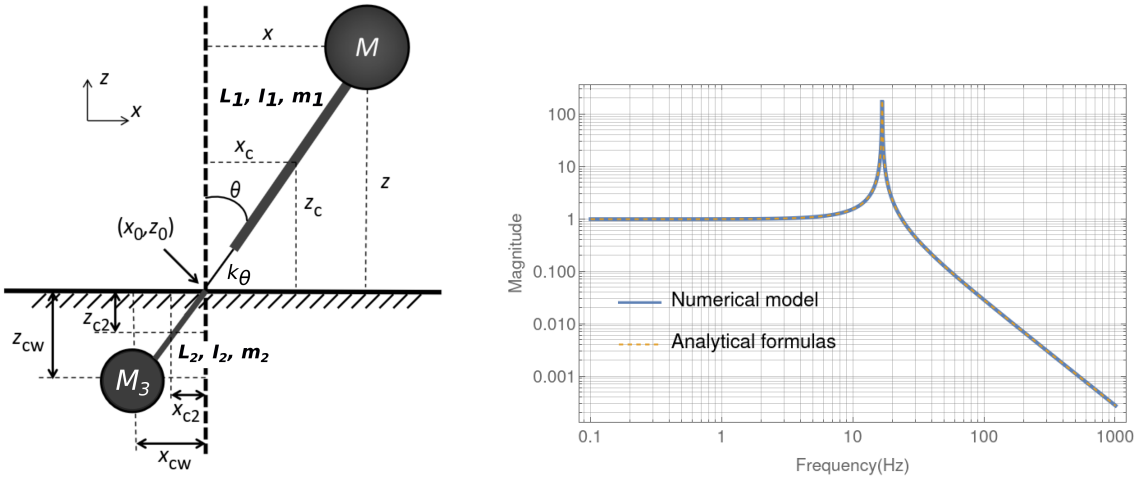

Figure 1: Left: One-dimensional model of an inverted pendulum. The diagram is adapted from Ref. [1, p.65]. Right: Transfer function magnitude of the lower body, calculated analytically and numerically. Both calculations coincide.

which allows us to write the transfer function as

$$H(s) = \frac{\omega_0 - \beta s^2}{\omega_0 + s^2}. \tag{6}$$

In the case of the cryogenic suspension, it is necessary to calculate the transfer function of the lower body $G(s)$ and optimize its saturation value β'. It is easy to show that

$$G(s) = 1 - \frac{L_2}{L_1}[H(s) - 1] = \frac{\omega_0 - \beta' s^2}{\omega_0 + s^2}, \tag{7}$$

Symbol	Value	Description
M	0.809 kg	Counterweight mass
L_1	0.525 m	Length of the beam holding the counterweight
m_1	0.612 kg	Mass of the beam holding the counterweight
I_1	0.014 kg m^2	Moment of inertia of the beam holding the counterweight
L_2	1.938 m	Length of the beam holding the load
m_2	2.258 kg	Mass of the beam holding the load
I_2	0.707 kg m^2	Moment of inertia of the beam holding the load
M_3	50 kg	Mass of the load

Table 1: The dimensions of the beams were read from the 3D-CAD and the masses and moments of inertia were calculated using a density value of $\rho = 2330\,\mathrm{kg/m^3}$.

where

$$\beta' = \frac{B'}{C}, \tag{8}$$

$$B' = -M\left(1+\frac{L_2}{L_1}\right) - \frac{m_1}{2}\left(\frac{L_2}{L_1}+\frac{1}{2}\right) + \frac{L_2^2 m_2}{4L_1^2} - \frac{I_1+I_2}{L_1^2} \tag{9}$$

$$\tag{10}$$

All the formulas above have been verified in two ways. First, they were calculated from scratch, and later, they were compared with a rigid body numerical simulation written in Modelica, using the MultiBody Library. For the sake of simplicity, the model does not take into account some of the features of the components, namely, the beam chamfer, the alcoves, the extra length of beam below the lower alcove and the mass and moment of inertia of the flexures. Fig. 1 shows on the right that the transfer functions provided by the formulas and the numerical model coincide. In this particular example, with a counterweight M = 0.808822 kg, the attenuation saturates at a value $\beta' \approx 1 \times 10^{-9}$ that does not appear in the plot. The values used for the parameters other than M, are also given in Table 1. A precision of milligrams, however, is not experimentally realistic. As will be done in Sec. 2, a realistic value is obtained by rounding off to the nearest tenth of a gram.

It is important to point out that the saturation value does not depend on the spring constant of the flexure k_θ, that only appears in the definition of the parameter A above. Therefore, it does not depend on the resonant frequency. In the example shown in Fig. 1, an arbitrary value of 16.65 Hz was chosen for the resonant frequency, but it will be adjusted based on the result of Finite Element Method analyses.

2 Results and discussion

As pointed out above, an experimentally feasible optimum value for the counterweight mass is set by rounding off the value in the example above to the nearest tenth of a gram $\mathrm{M_{opt}} = 0.8088$ kg. In practice, such a resolution can be achieved using droplets of Indium or Indium-Gallium alloy.

The plot on the left in Fig. 2 shows the saturation value β' as a function of the counterweight mass within ±10 g from the optimum value. The plot on the right depicts the magnitude of the transfer function $G(s)$ for different values of the mass. Namely, the value that makes β' nearly vanish, the optimum value, and this same value with the additions of 0.1, 1 and 10 g. In the case of the optimum value, the saturation becomes 1.5×10^{-7}, whereas for the cases in which 0.1, 1 and 10 g were added, it becomes 5×10^{-7}, 7×10^{-6} and 7×10^{-5} respectively. These results are summarized in Table 2 expressed as tolerances allowed in the mass adjustment.

Provided there are the means to measure the transfer function during assembly, it seems experimentally feasible to reach saturation values below 10^{-6} setting the tolerance for the mass to

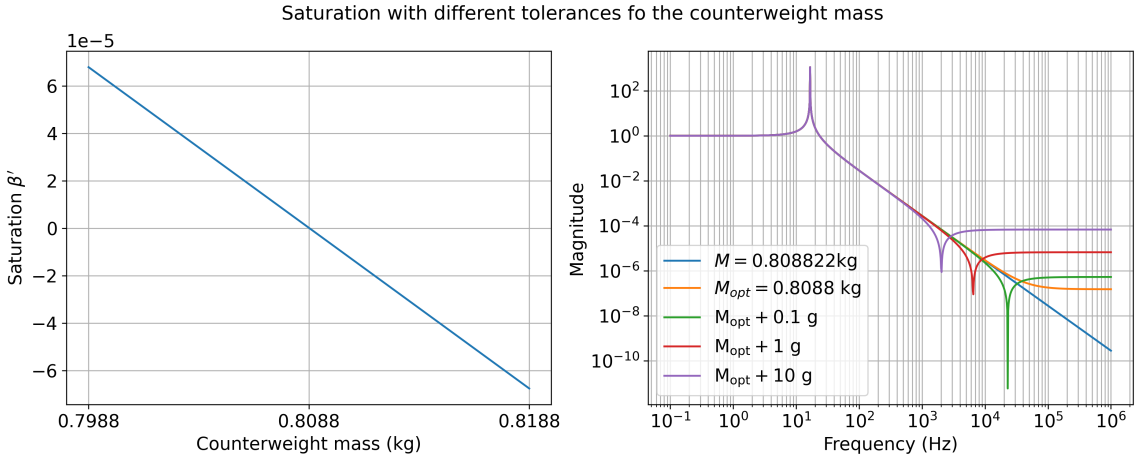

Figure 2: The plot on the left depicts the saturation value as a function of the counterweight mass within $\pm 10\,\mathrm{g}$ from the optimum value. The plot on the right shows the magnitude of the transfer function for different values of the mass.

Tolerance	**Saturation**
$\pm 0.1\,\mathrm{g}$	below 10^{-6}
$\pm 1\,\mathrm{g}$	below 10^{-5}
$\pm 10\,\mathrm{g}$	below 10^{-4}

Table 2: Upper limits of the saturation according to counterweight mass tolerance.

$\pm 0.1\,\mathrm{g}$. Despite this feasibility, the effect of the lower flexures must also be considered before setting a requirement for the saturation. These flexures provide additional vibration filtering such that any residual motion due saturation is rolled off above the second resonant frequency of the coupled system. Fig. 3 shows how the saturation rolls off when the counterweight mass is $10\,\mathrm{g}$ larger than the optimum value, and when it is completely absent. The calculation was done numerically in Modelica. The lower flexure was modelled as a spring constrained to move along the longitudinal direction, with a resonant frequency of a spring-mass (with M_3) system of 16.65 Hz.

Within the limits of this model, it seems the saturation produced by the physical properties of the beams could be set low enough for not harming the sensitivity of the interferometer.

References

[1] Mathieu Blom. “Seismic attenuation for Advanced Virgo Vibration isolation for the external injection bench”. PhD thesis. Vrije Universiteit Amsterdam, 2015. URL: `https://www.nikhef.nl/pub/services/biblio/theses_pdf/thesis_M_Blom.pdf`.

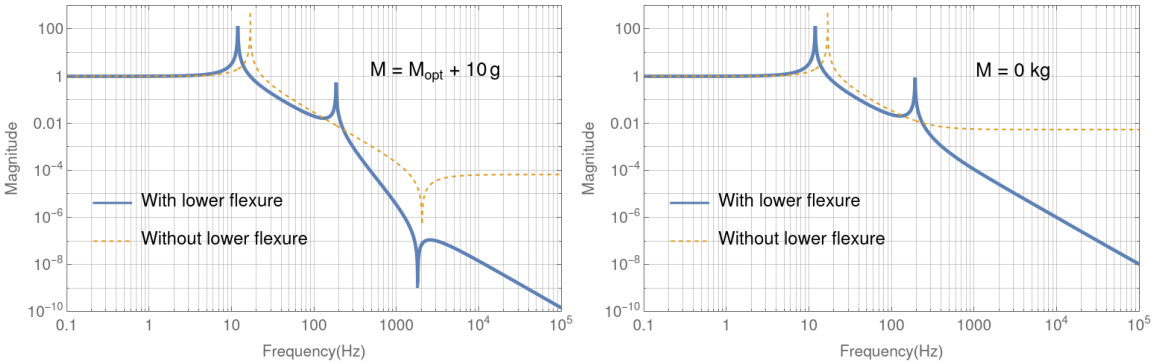

Figure 3: The saturation produced by the beam physical properties rolls off due to the effect of the lower flexures.

[2] Akiteru Takamori. "Low Frequency Seismic Isolation for Gravitational Wave Detectors". PhD thesis. University of Tokyo, 2002. URL: `https://granite.phys.s.u-tokyo.ac.jp/takamori/thesisver2002.pdf`.